Title

Toward high specific capacity and high cycling stability of pure tin nanoparticles with conductive polymer binder for sodium ion batteries

Authors

Dai, Kehua
Zhao, Hui
Wang, Zhihui
et al.

Publication Date

2014-10-01

DOI

10.1016/j.jpowsour.2014.04.012

Peer reviewed

Toward High Specific Capacity and High Cycling Stability of Pure Tin Nanoparticles with Conductive Polymer Binder for Sodium Ion Batteries

Abstract

Pure Sn nanoparticles electrode with Poly(9,9-dioctylfluorene-co-fluorenone-comethylbenzoic ester) (PFM) conductive binder are prepared and tested in sodium ion battery. It shows high specific capacity and high cycling stability without any conductive additive compared with Sn/CMC (carboxy methylated cellulose) and Sn/PVDF (polyvinylidene fluoride) electrode. The Sn in Sn/PFM electrodes delivers 806 mAh g^{-1} at C/50 and 610 mAh g^{-1} at C/10. After 10 cycles at C/10, the capacity of Sn has no decay. SEM and TEM images show that the Sn particles in Sn/PFM electrode are still fully coated by PFM polymer after huge expansion during sodiation and shrinkage during desodiation.

1. Introduction

Recently, more and more attention has been paid to sodium ion batteries due to the wide availability and low cost of sodium [1, 2]. There have been many kinds of cathode materials for sodium ion batteries [3-19]. However, it is still a huge challenge to develop a practical anode material with high specific capacity and high cycling stability. Graphite, which has been widely used in lithium ion batteries, do not work with sodium [20]. Although hard carbon can absorb Na atoms onto its surface thereby can be used as anode material for sodium ion batteries, its specific capacity (200~300 mAh/g) and density (~1.5 g/cm^3) are not satisfactory [20-23]. Metal oxide anode materials, such as sodium titanate or TiO_2, has lower specific capacity than hard carbon [24-32]. Intermetallic anode materials [33-38] (Si, Ge, Sn, Pb, Sb, etc.) have aroused much interest for their high

specific capacity. Si has a high capacity of 4200 mAh/g [39] but it also does not work in sodium ion batteries [40]. Thus among the intermetallic anode materials for sodium ion batteries, Sn seems to be a competitive candidate [40-45]. The theoretical specific capacity of Sn is about 847 mAh/g when assuming the full conversion into $Na_{15}Sn_4$ [43]. The density of β-Sn is 7.3 g/cm^3 so it also has high volumetric capacity. However, the pure Sn powder suffer big volume change in charge and discharge [44], so it is a significant challenge to improve the cycling stability of pure Sn.

In our previous works in lithium ion batteries, we point out that the polymer binder plays an important role in the cell's performance [46]. A conductive binder Poly(9,9-dioctylfluorene-co-fluorenone-comethylbenzoic ester) (PFM) designed by our group has been used in Si and Sn anode material for lithium ion battery [47-49]. It is a polyfluorene-type polymer with two key function groups—carbonyl and methylbenzoic ester—for tailoring the polymer to be conductive in the cycling potential range and for improving the mechanical binding force, respectively. With this binder, the pure Sn nanoparticles exhibit high cycling stability besides high specific capacity in lithium ion battery [48]. However, Na^+ has bigger ionic radius than Li^+, so the volume expansion of Sn during sodiation is bigger than during lithiation (430% vs. 300%). The PFM binder faces bigger challenge in the sodium system. In this work, we prepared Sn/PFM composed electrode without any conductive additive, then examined its electrochemical performance and compared it with Sn/CMC (carboxy methylated cellulose) and Sn/PVDF (polyvinylidene fluoride) electrode.

2. Experimental

The design, preparation, characterization and simulation of conductive polymer can be found in our published paper [49]. Sn nanoparticles were purchased from Sigma-Aldrich. The particle size defined by the company is <150 nm and the purity is over 99% by metal Sn content. Defined amount of Sn nanoparticles were dispersed in the conductive polymer PFM chlorobenzene solution to form a slurry. For comparison, same Sn nanoparticles were also dispersed in CMC water or PVDF NMP solutions to form slurries. The slurries were doctor-bladed onto copper foil, dried at room temperature, then was punched into discs (diameter = 13 mm) and was dried at 90 °C for 12 h in a vacuum oven. The weight ratios of Sn/PFM, Sn/CMC and Sn/PVDF were 95/5, 95/5 and 98/2, respectively. 2325 coin cells were fabricated with the Sn electrodes, sodium foil, 1 mol L^{-1} $NaClO_4$ in 7/3 propylene carbonate (PC)/fluoroethylene carbonate (FEC), and two-layered Celgard 2400 polypropylene separator. The coin cells were assembled in an argon-filled glove box and galvanostatic charge-discharge tests were performed using Maccor 4000 at 30 °C. The voltage range was 0.8-0 V. The morphology of the electrodes were examined using a JEOL 7500F scanning electron microscope (SEM) and a Philips CM200FEG transmission electron microscopy (TEM).

3. Results and discussion

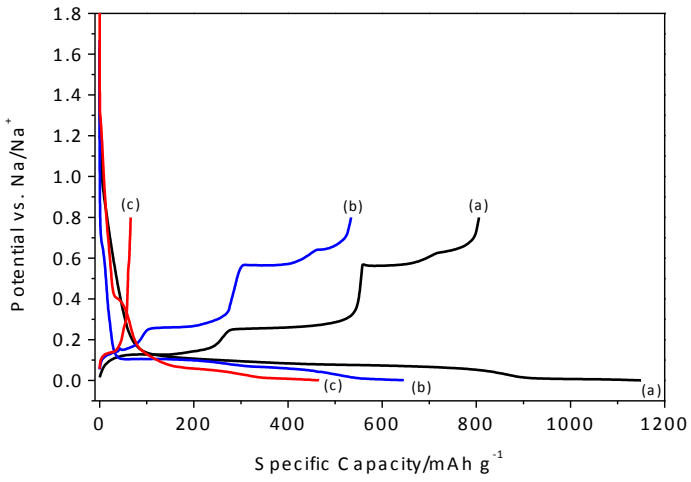

Fig. 1. The first charge and discharge profiles of (a) Sn/PFM, (b) Sn/CMC and (c) Sn/PVDF. The charge and discharge rate is C/50 (16 mA g^{-1})

Fig. 1 shows the first charge and discharge profiles of the three electrode. The charge capacities of Sn/PFM, Sn/CMC and Sn/PVDF are 806 mAh g^{-1}, 533 mAh g^{-1}, 65.7 mAh g^{-1}, respectively. The Sn/PFM has the highest charge capacity, which is near the theoretical capacity of Sn (847 mAh g^{-1}). We believe this is benefited by the conductivity of PFM polymer. The Sn/CMC has the medium capacity, this is because although the conductivity of CMC is weaker than that of PFM, the Na^+ ion in CMC is helpful for Na^+ ion transfer. The charge capacity of Sn/PVDF is very poor for the electric insulativity of PVDF. The charge profiles of Sn/PFM has four voltage plateau: 0.13 V, 0.25 V, 0.56V and 0.63 V, which are refer to two-phase reactions of $Na_{15}Sn_4$-Na_9Sn_4, Na_9Sn_4-NaSn, NaSn-$NaSn_5$ and $NaSn_5$-Na, respectively [42-44]. The ration of plateau length is near to theoretical calculating value [41]. Although the charge profiles of Sn/CMC also has four similar voltage plateau, and the length of the two higher voltage plateau is close to that of Sn/PFM, the two lower voltage plateau is much shorter than that of Sn/PFM. As the lower voltage, the higher volume expansion, this difference of voltage plateau suggests that when Sn particles become rather big, the CMC cannot completely bind all the Sn

particles. The discharge capacity of Sn/PFM is over the theoretical capacity of Sn. This might because Sn is consumed in SEI formation and partly absorbed by polymer.

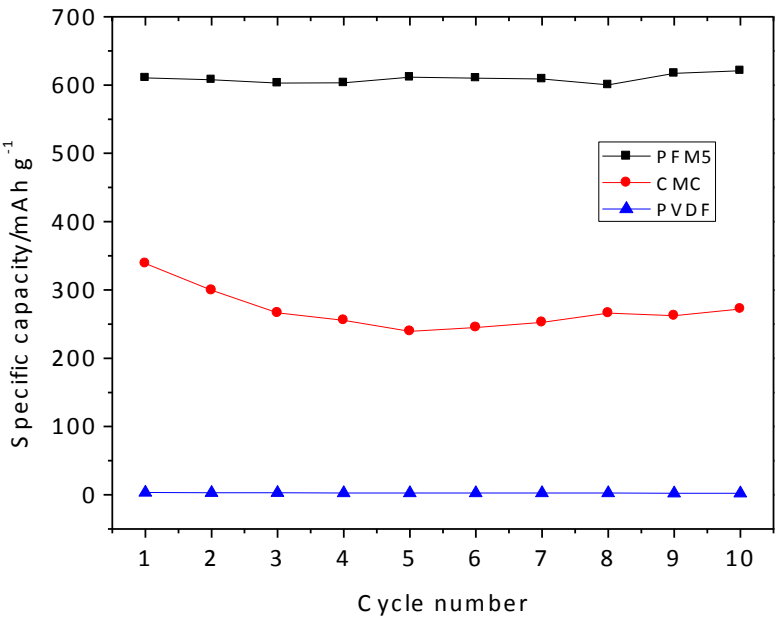

Fig. 2. The charge capacity vs. cycle number of Sn/PFM, Sn/CMC and Sn/PVDF. The charge and discharge rate is C/10 (80 mA g^{-1})

Fig.2 exhibits the cycling stability of Sn/PFM, Sn/CMC and Sn/PVDF. Firstly, at C/10, the initial charge capacity of Sn/PFM is 610 mAh g^{-1}, amount to 75.7% of capacity at C/50, which is higher than previous result (less than 500 mAh g^{-1}, Sn 80%, carbon black 10%, PAA 10%, 50 mA g^{-1} [40]). However, the ratios of capacities at C/10 and C/50 are only 63.6% and 5.3% for Sn/CMC and Sn/PVDF, respectively, so Sn/PFM shows the best rate performance. Secondly, the capacity of Sn/PFM is very stable along cycling. After 10 cycles, the capacity is still 621 mAh g^{-1}, and has no decay. Comparatively, the capacity of Sn/CMC decreases fast at the first 5 cycles then increases slightly at the following 5 cycles. The capacity retention of Sn/CMC is only 80% after 10 cycles. The

excellent cycling stability of Sn/PFM anode electrode in sodium ion battey is believed originate in the conductivity and strong adhesion of PFM conductive binder.

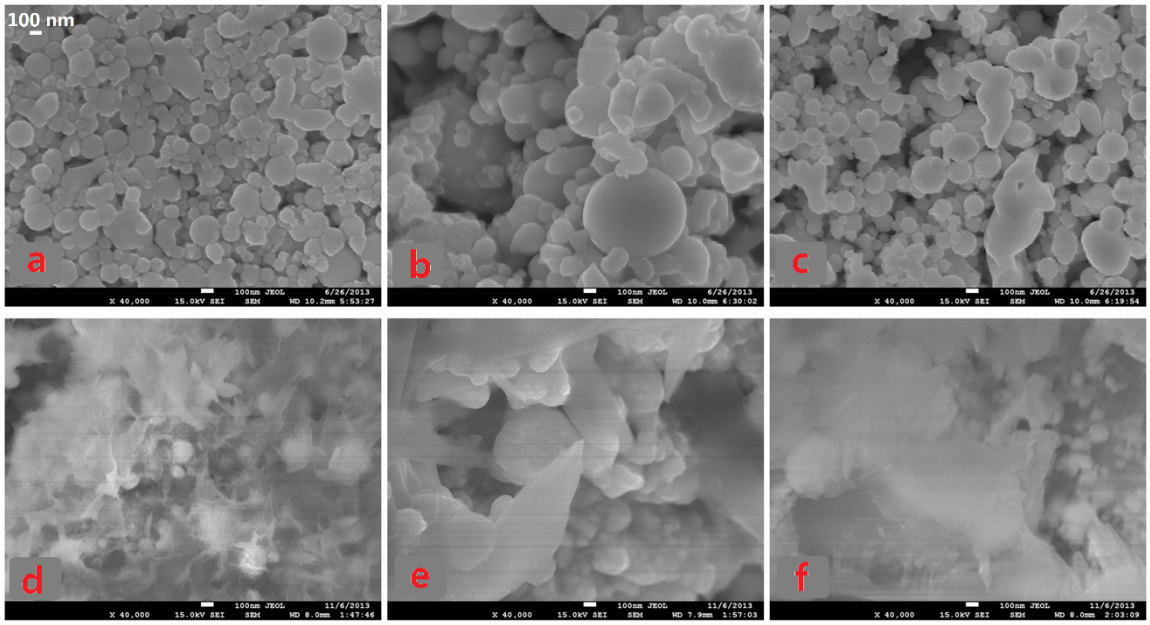

Fig. 3. SEM images of the electrodes: (a) pristine Sn/PFM; (b) pristine Sn/CMC; (c) pristine Sn/PVDF; (d) Sn/PFM after 1 cycle; (e) Sn/CMC after 1 cycle; (f) Sn/PVDF after 1 cycle.

Fig. 3 shows the morphology of the pristine and after-1-cycle electrodes. The three pristine electrodes of different composition have similar morphology. Polymer is hardly found in the images because the polymer is uniformly coated onto the surface of particles. However, in the first cycle, because the Sn particles expand during sodiation and then shrink again during desodiation, the three electrodes of different composition after 1 cycle show much difference. The Sn particles in Sn/PFM electrode still bind closely to PFM polymer, but those in Sn/CMC and Sn/PVDF electrodes separate from polymer. This agrees with the analysis on the voltage plateau of Sn/PFM and Sn/CMC.

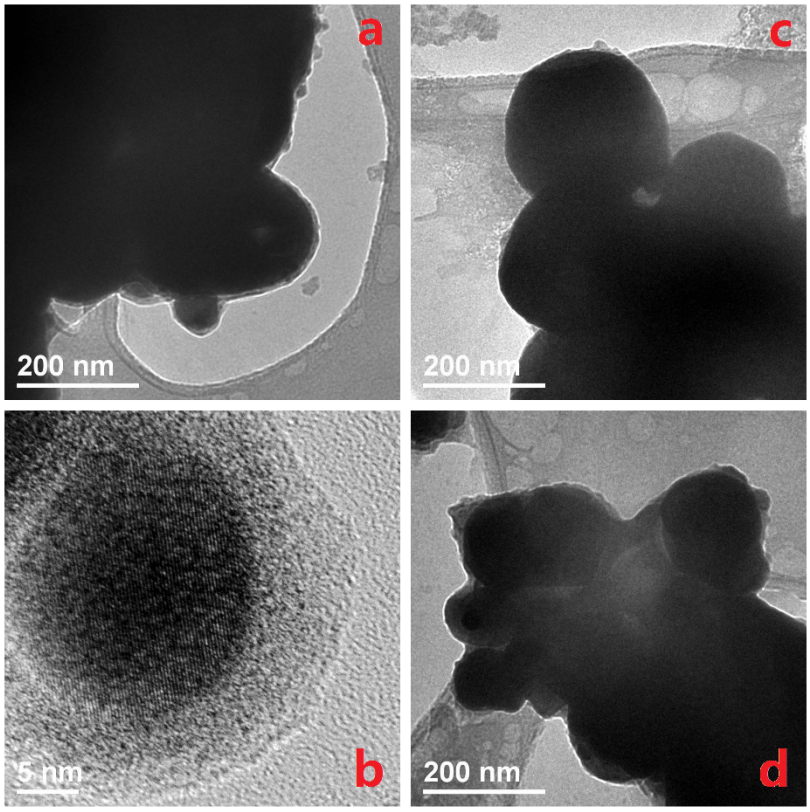

Fig. 4 TEM images of the electrodes: (a) (b) Sn/PFM after 1 cycle; (c) Sn/CMC after 1 cycle; (d) Sn/PVDF after 1 cycle.

Fig.4 is the TEM images of the three electrodes of different composition after 1 cycle. From (a), (c) and (d) it can be seen that the Sn particles in Sn/PFM electrode are fully coated by PFM polymer, but the coating of polymer on the surface of Sn particles in Sn/CMC and Sn/PVDF electrodes is not completed. Fig. 4 (b) shows high resolution image of a Sn particle in the Sn/PFM electrode after 1 cycle. The inner circle zone with lattice is Sn, and the outer ring zone without lattice is PFM polymer. The polymer coating is perfect. The thickness of polymer is 7~9 nm, which agrees with our previous calculation[48].

4. Conclusion

The electrode composed by pure Sn nanoparticles and PFM conductive polymer shows high specific capacity and high cycling stability without any conductive additive. The Sn in Sn/PFM electrodes delivers 806 mAh g^{-1} at C/50 and 610 mAh g^{-1} at C/10. After 10 cycles at C/10, the capacity of Sn has no decay. SEM and TEM images show that the Sn particles in Sn/PFM electrode are still fully coated by PFM polymer after huge expansion during sodiation and shrinkage during desodiation.

[1] M.D. Slater, D. Kim, E. Lee, C.S. Johnson, Adv Funct Mater, 23 (2013) 947-958.
[2] B.L. Ellis, L.F. Nazar, Curr Opin Solid St M, 16 (2012) 168-177.
[3] P. Barpanda, T. Ye, S. Nishimura, S.C. Chung, Y. Yamada, M. Okubo, H.S. Zhou, A. Yamada, Electrochem Commun, 24 (2012) 116-119.
[4] N. Bucher, S. Hartung, I. Gocheva, Y.L. Cheah, M. Srinivasan, H.E. Hoster, J Solid State Electr, 17 (2013) 1923-1929.
[5] K. Chihara, A. Kitajou, I.D. Gocheva, S. Okada, J. Yamaki, J Power Sources, 227 (2013) 80-85.
[6] J.J. Ding, Y.N. Zhou, Q. Sun, Z.W. Fu, Electrochem Commun, 22 (2012) 85-88.
[7] J.J. Ding, Y.N. Zhou, Q. Sun, X.Q. Yu, X.Q. Yang, Z.W. Fu, Electrochim Acta, 87 (2013) 388-393.
[8] K.H. Ha, S.H. Woo, D. Mok, N.S. Choi, Y. Park, S.M. Oh, Y. Kim, J. Kim, J. Lee, L.F. Nazar, K.T. Lee, Adv Energy Mater, 3 (2013) 770-776.
[9] Z.L. Jian, W.Z. Han, X. Lu, H.X. Yang, Y.S. Hu, J. Zhou, Z.B. Zhou, J.Q. Li, W. Chen, D.F. Chen, L.Q. Chen, Adv Energy Mater, 3 (2013) 156-160.
[10] Z.L. Jian, H.J. Yu, H.S. Zhou, Electrochem Commun, 34 (2013) 215-218.
[11] Z.L. Jian, L. Zhao, H.L. Pan, Y.S. Hu, H. Li, W. Chen, L.Q. Chen, Electrochem Commun, 14 (2012) 86-89.
[12] J. Kang, S. Baek, V. Mathew, J. Gim, J. Song, H. Park, E. Chae, A.K. Rai, J. Kim, J Mater Chem, 22 (2012) 20857-20860.
[13] R. Kataoka, T. Mukai, A. Yoshizawa, T. Sakai, J Electrochem Soc, 160 (2013) A933-A939.
[14] S.W. Kim, D.H. Seo, X.H. Ma, G. Ceder, K. Kang, Adv Energy Mater, 2 (2012) 710-721.
[15] M. Nose, S. Shiotani, H. Nakayama, K. Nobuhara, S. Nakanishi, H. Iba, Electrochem Commun, 34 (2013) 266-269.
[16] J.F. Qian, X.Y. Wu, Y.L. Cao, X.P. Ai, H.X. Yang, Angew Chem Int Edit, 52 (2013) 4633-4636.
[17] J.F. Qian, M. Zhou, Y.L. Cao, X.P. Ai, H.X. Yang, Adv Energy Mater, 2 (2012) 410-414.
[18] P. Serras, V. Palomares, A. Goni, P. Kubiak, T. Rojo, J Power Sources, 241 (2013) 56-60.
[19] J.A. Saint, M.M. Doeff, J. Wilcox, Chem Mater, 20 (2008) 3404-3411.
[20] D.A. Stevens, J.R. Dahn, J Electrochem Soc, 147 (2000) 1271-1273.
[21] R. Alcantara, J.M. Jimenez-Mateos, P. Lavela, J.L. Tirado, Electrochem Commun, 3 (2001) 639-642.

[22] W. Luo, J. Schardt, C. Bommier, B. Wang, J. Razink, J. Simonsen, X.L. Ji, J Mater Chem A, 1 (2013) 10662-10666.
[23] A. Ponrouch, A.R. Goni, M.R. Palacin, Electrochem Commun, 27 (2013) 85-88.
[24] Z.H. Bi, M.P. Paranthaman, P.A. Menchhofer, R.R. Dehoff, C.A. Bridges, M.F. Chi, B.K. Guo, X.G. Sun, S. Dai, J Power Sources, 222 (2013) 461-466.
[25] J.P. Huang, D.D. Yuan, H.Z. Zhang, Y.L. Cao, G.R. Li, H.X. Yang, X.P. Gao, Rsc Adv, 3 (2013) 12593-12597.
[26] A. Rudola, K. Saravanan, S. Devaraj, H. Gong, P. Balaya, Chem Commun, 49 (2013) 7451-7453.
[27] P. Senguttuvan, G. Rousse, V. Seznec, J.M. Tarascon, M.R. Palacin, Chem Mater, 23 (2011) 4109-4111.
[28] Y. Sun, L. Zhao, H.L. Pan, X. Lu, L. Gu, Y.S. Hu, H. Li, M. Armand, Y. Ikuhara, L.Q. Chen, X.J. Huang, Nat Commun, 4 (2013).
[29] W. Wang, C.J. Yu, Z.S. Lin, J.G. Hou, H.M. Zhu, S.Q. Jiao, Nanoscale, 5 (2013) 594-599.
[30] W. Wang, C.J. Yu, Y.J. Liu, J.G. Hou, H.M. Zhu, S.Q. Jiao, Rsc Adv, 3 (2013) 1041-1044.
[31] H. Xiong, M.D. Slater, M. Balasubramanian, C.S. Johnson, T. Rajh, J Phys Chem Lett, 2 (2011) 2560-2565.
[32] Y. Xu, E.M. Lotfabad, H.L. Wang, B. Farbod, Z.W. Xu, A. Kohandehghan, D. Mitlin, Chem Commun, 49 (2013) 8973-8975.
[33] L. Baggetto, E. Allcorn, R.R. Unocic, A. Manthiram, G.M. Veith, J Mater Chem A, 1 (2013) 11163-11169.
[34] L. Baggetto, J.K. Keum, J.F. Browning, G.M. Veith, Electrochem Commun, 34 (2013) 41-44.
[35] M.K. Datta, R. Epur, P. Saha, K. Kadakia, S.K. Park, P.N. Kuma, J Power Sources, 225 (2013) 316-322.
[36] L. Wu, P. Pei, R.J. Mao, F.Y. Wu, Y. Wu, J.F. Qian, Y.L. Cao, X.P. Ai, H.X. Yang, Electrochim Acta, 87 (2013) 41-45.
[37] Y.H. Xu, Y.J. Zhu, Y.H. Liu, C.S. Wang, Adv Energy Mater, 3 (2013) 128-133.
[38] T.T. Tran, M.N. Obrovac, J Electrochem Soc, 158 (2011) A1411-A1416.
[39] C.K. Chan, H.L. Peng, G. Liu, K. McIlwrath, X.F. Zhang, R.A. Huggins, Y. Cui, Nat Nanotechnol, 3 (2008) 31-35.
[40] S. Komaba, Y. Matsuura, T. Ishikawa, N. Yabuuchi, W. Murata, S. Kuze, Electrochem Commun, 21 (2012) 65-68.
[41] V.L. Chevrier, G. Ceder, J Electrochem Soc, 158 (2011) A1011-A1014.
[42] L.D. Ellis, T.D. Hatchard, M.N. Obrovac, J Electrochem Soc, 159 (2012) A1801-A1805.
[43] M. Mortazavi, J.K. Deng, V.B. Shenoy, N.V. Medhekar, J Power Sources, 225 (2013) 207-214.
[44] L. Baggetto, P. Ganesh, R.P. Meisner, R.R. Unocic, J.C. Jumas, C.A. Bridges, G.M. Veith, J Power Sources, 234 (2013) 48-59.
[45] H.L. Zhu, Z. Jia, Y.C. Chen, N. Weadock, J.Y. Wan, O. Vaaland, X.G. Han, T. Li, L.B. Hu, Nano Lett, 13 (2013) 3093-3100.
[46] G. Liu, H. Zheng, X. Song, V.S. Battaglia, J Electrochem Soc, 159 (2012) A214-A221.
[47] S.D. Xun, B. Xiang, A. Minor, V. Battaglia, G. Liu, J Electrochem Soc, 160 (2013) A1380-A1383.
[48] S.D. Xun, X.Y. Song, V. Battaglia, G. Liu, J Electrochem Soc, 160 (2013) A849-A855.
[49] G. Liu, S.D. Xun, N. Vukmirovic, X.Y. Song, P. Olalde-Velasco, H.H. Zheng, V.S. Battaglia, L.W. Wang, W.L. Yang, Adv Mater, 23 (2011) 4679-4683.